PHYSICAL REVIEW B VOLUME 39, NUMBER 7 1 MARCH 1989

Tight-binding Hamiltonians for high-temperature superconductors and applications to coherent-potential-approximation calculations of the electronic properties of $La_{2-x}Ba_xCuO_{4-y}$

M. J. DeWeert, D. A. Papaconstantopoulos, and W. E. Pickett
Complex Systems Theory Branch, Naval Research Laboratory, Code 4690, Washington, D.C. 20375
(Received 4 November 1988)

We present accurate tight-binding parametrizations of the first-principles augmented-plane-wave or linearized-augmented-plane-wave band structures of $LaCuO_3$, La_2CuO_4, Ba_2CuO_4, and the high-temperature superconductor $YBa_2Cu_3O_7$. We discuss the methodology and efficient application of these fits, including as an example our tight-binding coherent-potential-approximation (CPA) calculations of the effects of disorder on the electronic structure of $La_{2-x}Ba_xCuO_{4-y}$. Our CPA calculations support the hypothesis of a rigid-band lowering of the Fermi level for $La_{2-x}Ba_xCuO_4$, enhancing the density of states there. However, for La_2CuO_{4-y} they yield the interesting result that oxygen vacancies *also* lower E_F and raise $N(E_F)$. This is a significant result for the theory of superconductivity in these materials. In addition to CPA calculations, our parametrizations of the band structures should prove to be a useful tool for other studies which will enhance our understanding of these materials.

I. INTRODUCTION

Since the discovery of ceramics which display high-temperature superconductivity, these systems have been under intense theoretical and experimental investigation. Several studies[1-4] have dealt with band structures of ordered materials, and comparisons to experimental results indicate that disorder and correlations play an important role in these materials. For example,[5] La_2CuO_4 exhibits a transition from an antiferromagnetic insulating state to a superconducting state as La is replaced by Ba or Sr. An important adjunct to extending our understanding of these compounds is their parametrization in terms of tight-binding models.

A tight-binding model can be used to give insight into difficult problems, and is compact enough to be easily used to study problems which are intractable with standard *ab initio* techniques or beyond their scope. For example, it allows one to consider impurities and concentrated alloys,[6] phonon spectra, and the electron-phonon interaction.[7] It can be used as a starting point for many-body calculations, such as the $1/N$ expansions[8] which have been used to understand the Anderson lattice Hamiltonian model for $La_{2-x}Sr_xCuO_4$. Regardless of the actual theory of superconductivity which applies to this class of materials, our parametrizations can be an important tool, and other investigations will be aided by the availability of our work.

In this paper, we will confine our discussion to $LaCuO_3$, $La_{2-x}Ba_xCuO_{4-y}$, and $YBa_2Cu_3O_7$. Many investigators[9,10] have proposed simplified models based on isolated copper-oxygen planes. We present here accurate *three*-dimensional (3D) parametrizations and their applications to two problems which are extremely difficult to do with *ab initio* techniques: substitutional disorder in rare-earth sites and disordered vacancies in oxygen sites of La_2CuO_4.

Stoichiometric La_2CuO_4 is observed to be an antiferromagnetic insulator, but substituting Ba for La causes a transition to superconducting behavior for as little as 3 at.% Ba.[11] One speculation is that disorder frustrates the antiferromagnetic state of the pure compound, allowing the paramagnetic local-density-approximation (LDA) band structure to assert itself. If this is true, then we need only account for impurity scattering to understand the properties of the alloy. On the other hand, it has also been suggested that disorder alone is not sufficient to make La_2CuO_4 metallic, and that the failure is in the LDA's treatment of electron self-interactions. If this is the case, self-interaction corrections[12] need to be included to determine the band structure of the stoichiometric material before the effects of impurities and defects can be considered. We will not address the latter speculation, but will demonstrate in this paper that the former hypothesis leads to a dependence of the density of states (DOS) at the Fermi surface on x for $La_{2-x}Ba_xCuO_4$ which is consistent with the rise of T_c as x increases. We will also demonstrate that oxygen vacancies can play a role similar to that of barium substitutions.

II. SLATER-KOSTER FITS FOR CERAMIC SUPERCONDUCTORS

A. General

The Slater-Koster (SK) method[13] treats tight-binding (TB) matrix elements and overlap integrals as disposable constants to be determined by fitting the TB band structure to a first-principles calculation. We have performed augmented-plane-wave[14] (APW) or linearized-augmented-plane-wave[1,2] (LAPW) calculations to generate eigenvalues $E_n(k)$ and angular momentum components $Q_{nlm}(k)$ for the materials considered here: $LaCuO_3$, La_2CuO_4, Ba_2CuO_4, and $YBa_2Cu_3O_7$. By angular

momentum component $Q_{nlm}(k)$, we mean the fraction of electronic charge in the nth band for the lth angular momentum component of the mth basis atom. These components are normalized so that the sum over l and m of the Q's is unity at each k vector for each energy level, and this quantity is used to decompose the DOS. In practice, we approximate the Q's for the (L)APW calculations by that part of the charge inside the muffin-tin spheres. In the Slater-Koster fits, we identify $Q_{nlm}(k)$'s as squares of norms of coefficients of the expansions of TB wave functions in terms of atomiclike orbitals. These also sum to unity for each band at each momentum.

The inclusion of angular momentum information is an important innovation in our work. Given only $E_n(k)$ data, we find that even for the relatively simple cubic oxide $LaCuO_3$, we cannot generate TB bands with the proper angular momentum characters. Specifically, copper d bands and oxygen p bands may not be well distinguished from one another in a fit performed without angular momentum information. This reflects the high degree of Cu-O hybridization characteristic of this class of compounds. One way to facilitate the fitting is to use the symmetry of the bands. However, we do not have this symmetry information readily available in our codes, and we have also found it necessary to fit points of no symmetry to insure a high-quality fit throughout the zone.

Accordingly, the functional F we minimize is $F=\sum_{k,n}[f_n(k)]^2$, where

$$f_n(k)=|E_n^{\mathrm{APW}}(k)-E_n^{\mathrm{SK}}(k)| + \sum_j |Q_{n,j}^{\mathrm{APW}}(k)-Q_{n,j}^{\mathrm{SK}}(k)|/W ,$$

where the superscripts APW and SK denote the first-principles and Slater-Koster values, respectively. Here, the index j combines indices for atom kind and angular momentum character. W is a weight used to adjust the relative importance of $E_n(k)$ and $Q_{nj}(k)$ in our fits. Since E is in rydbergs and Q is dimensionless, the choice of W is not obvious. To obtain our fits, we use $W=10$ for $LaCuO_3$, $W=4$ for La_2CuO_4 and Ba_2CuO_4, and $W=200$ for $YBa_2Cu_3O_7$.

We restrict our bases to include at most s, p, and d bands for Cu and the cations, and to include at most s and p for O. Though the cations do contribute significant f density,[1] it is generally well above E_F, so we have neglected it. All of the fits discussed in this paper are done in the two-center approximation with orthogonal bases. We prefer orthogonal bases because they facilitate construction of Green's functions to be used in CPA calculations.

It is necessary for the correct interpretation of our tables of parameters to define the notation clearly. A general overlap integral for atom pair A,A' has the form $(ll'\alpha)$, where $l,l'=s,p,d,\ldots$ represent the angular momentum of the states on A and A', respectively, and $\alpha=\sigma,\pi,\delta,\ldots$ specifies the azimuthal quantum number $0,1,2,\ldots$ with respect to the axis joining the pair of atoms. Representing this parameter by $(ll'\alpha)_{AA'}$, the parity of the states leads to the relation $(ll'\alpha)_{AA'}=(-1)^{l+l'}(l'l\alpha)_{AA'}$.

As an example, we clarify the important "Cu-O $(pd\sigma)$" overlap integral, as it is often called. This should be properly called the "O-Cu $(pd\sigma)$" parameter, which describes the hopping for O p states to Cu d states *with oxygen taken as the reference atom* (p first). In our tables, we actually present the Cu-O $(dp\sigma)$ parameter, which *differs by a sign:* $(dp\sigma)_{\mathrm{Cu\text{-}O}}=-(pd\sigma)_{\mathrm{O\text{-}Cu}}$. This must be taken into account when comparing fits by different groups, and often this convention is not followed in the literature.

TABLE I. Coordinates of atoms for $LaCuO_3$. (Units of $a=7.8234$ a.u.)

Atom	x	y	z
La	0.50	0.50	0.50
Cu	0.00	0.00	0.00
O	0.50	0.00	0.00
O	0.00	0.50	0.00
O	0.00	0.00	0.50

B. $LaCuO_3$

Though this material is not itself superconducting, we consider it because it is a building block for the high-T_c superconductors. We take the structure to be cubic, with a lattice constant $a=7.8234$ a.u. The coordinates of the atoms in the unit cell are given in Table I. In our SK fit, we include La s and d; Cu s, p, and d; and O p states, giving us a 24×24 secular equation. The hopping matrix elements are restricted to first neighbors, and the neighbor distances are listed in Table II.

We have fit 19 APW bands at 35 k points to obtain an overall rms error of 11.7 mRy for the energies. The 42 TB parameters obtained are listed in Table III. Several of the hopping parameters, especially those associated with hopping within the Cu-O planes, are quite large, in the range of 0.1 Ry. This is reflected in the large width of the Fermi-level crossing $\mathrm{Cu}(x^2-y^2)$-$\mathrm{O}(p_{x,y})$ band, and is a feature common to all of the fits discussed in this paper.

As mentioned in the previous section, we have also performed an SK fit which does not account for the angular momentum decomposition of the bands. It gives accurate $E_n(k)$ values, but yields poor partial DOS when compared to first-principles results. By contrast, the inclusion of angular momentum information allows us to distinguish Cu d bands from O p bands, as is illustrated in Fig. 1, which shows decomposed DOS for the Cu d bands and O p bands, together with the total. The decomposition agrees well with the APW result, demonstrating the usefulness of including the decomposition in the fit. The SK fits included no La f states, but we have plotted the La d densities to show that they are negligible in the fit for the energies of interest.

TABLE II. Neighbor distances for $LaCuO_3$ (units of a).

First neighbors	La	Cu	O
La	1.000	0.866	0.707
Cu		1.000	0.500
O			0.707

TABLE III. Orthogonal TB parameters (42 total) for $LaCuO_3$, in rydbergs.

		On-site parameters			
La:	s	0.9713	Cu:	s	1.1049
	t_{2g}	0.8009		p	1.5545
	e_g	0.7553		t_{2g}	0.2031
O:	p	0.2334		e_g	0.2309
		First-neighbor parameters			
La-La:	$ss\sigma$	0.0137	Cu-Cu:	$ss\sigma$	0.0406
	$sd\sigma$	−0.0147		$sp\sigma$	0.0796
	$dd\sigma$	−0.0270		$pp\sigma$	−0.1928
	$dd\pi$	−0.0076		$pp\pi$	0.0293
	$dd\delta$	−0.0099		$sd\sigma$	0.0157
La-Cu:	$ss\sigma$	−0.0738		$pd\sigma$	−0.0084
	$sp\sigma$	−0.0676		$pd\pi$	0.0001
	$sd\sigma$	0.0298		$dd\sigma$	−0.0075
	$dd\sigma$	0.0302		$dd\pi$	−0.0014
	$dd\pi$	0.0055		$dd\delta$	−0.0050
	$dd\delta$	−0.0046	Cu-O:	$sp\sigma$	−0.0938
	$ds\sigma$	0.0316		$pp\sigma$	0.0658
	$dp\sigma$	0.0544		$pp\pi$	0.0324
	$dp\pi$	−0.0890		$dp\sigma$	0.0387
La-O:	$sp\sigma$	0.0499		$dp\pi$	0.0331
	$dp\sigma$	0.4877	O-O:	$pp\sigma$	0.0382
	$dp\pi$	0.0599		$pp\pi$	−0.0004

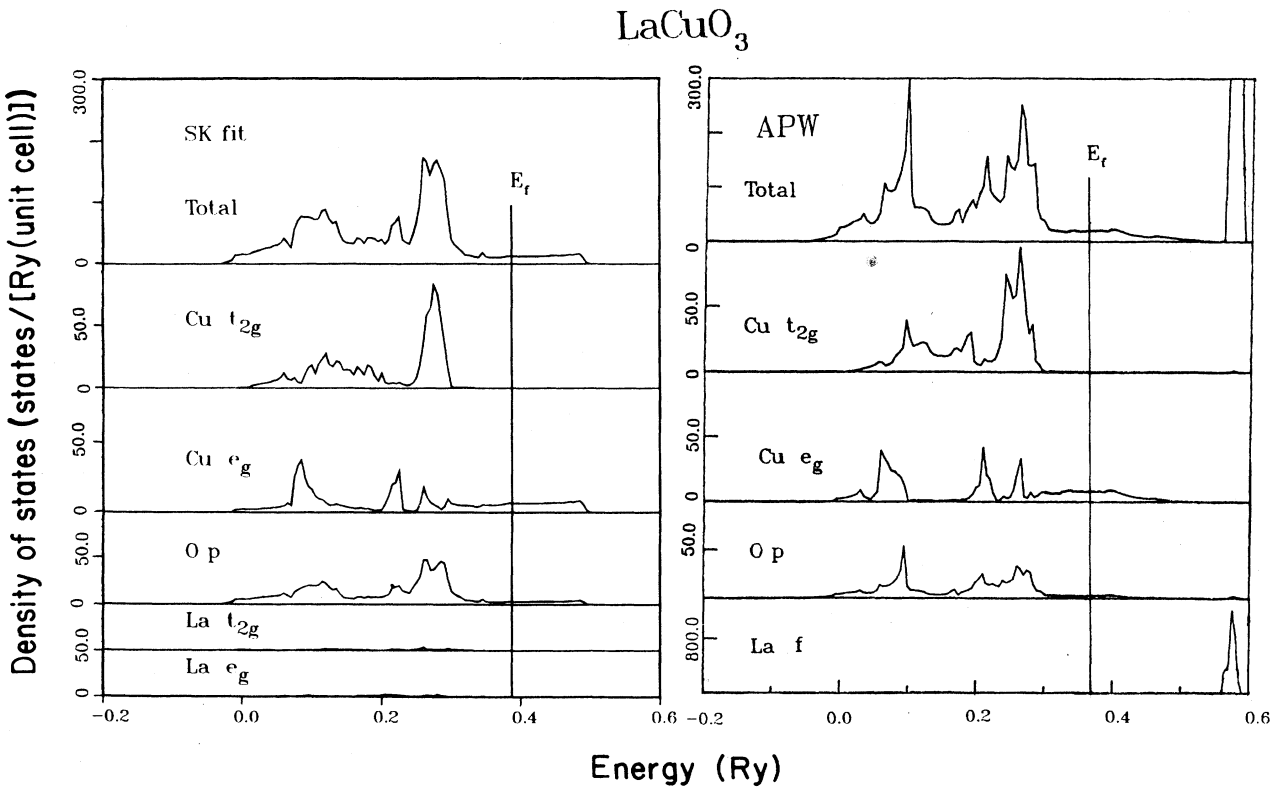

FIG. 1. $LaCuO_3$: APW vs SK fit for the total DOS and selected decomposed densities.

TABLE IV. La_2CuO_4 (Ba_2CuO_4) structure. For both compounds, $a=7.1622$ a.u. and $c/2a=1.74272$.

Atom	x (units of a)	y (units of a)	z (units of $c/2$)
La(Ba)	0.50	0.50	0.275
La(Ba)	0.00	0.00	0.724
Cu	0.00	0.00	0.00 plane
O(1)	0.50	0.00	0.00 plane
O(1)	0.00	0.50	0.00 plane
O(2)	0.00	0.00	0.364
O(2)	0.50	0.50	0.636

The densities of states presented in Figs. 1, 4, 5(a), 5(b), 7, 8, and 10 were calculated using the well-known linear tetrahedron method. When very precise comparisons need to be made between SK and first-principles total DOS, as in La_2CuO_4, we use exactly the same k points for the two calculations. For comparison of *decomposed* DOS here and below, it should be remembered that very close agreement should not be expected, since the decompositions are not performed on identical basis sets. For the (L)APW calculations, only the volume inside the muffin-tin spheres is decomposed, into an angular momentum expansion around the atom. However, the SK decomposition amounts to a projection onto Löwdin orbitals and includes *all* space. Small discrepancies are to be expected even in the case of a perfect SK fit.

C. La_2CuO_4 and Ba_2CuO_4

A preliminary report on our fit for La_2CuO_4 has been presented elsewhere.[15] We now present more details of these calculations.

For these compounds, we consider again first-neighbor interactions for each atom pair. Table IV gives the coordinates of the atoms, and Table V the neighbor distances. For the cation to cation (La-La and Ba-Ba) hopping elements we use identical hopping matrix elements for first and second neighbors, since the distances differ by only 5% of the a-axis length. We include La(Ba) d; Cu s, p, and d; and O p states, giving a 31×31 secular equation.

The lack of local cubic symmetry complicates SK fits for these compounds. Site symmetry dictates that directions x and y are distinct from z for La, Cu, and O(2), and x, y, and z are all distinct for O(1). In principle, this leads to crystal-field splittings in the on-site parameters for the d and p bands. With these splittings included, we would have five more on-site SK parameters than cubic symmetry would require. However, we find that splittings beyond those appropriate to cubic symmetry are very small and improve the fit by only a fraction of a mRy overall. We thus neglect them, considering the p states to be unsplit, and the Cu d states to be split as $t_{2g}(xz, yz,$ and $xy)$ and $e_g(x^2-y^2$ and $3z^2-r^2)$.

TABLE V. Neighbor distances for La_2CuO_4 (Ba_2CuO_4) in units of a. (* indicates that parameters for neighbors at $1.05a$ were the same as for this neighbor.)

First neighbors	La(Ba)	Cu	O(1)	O(2)
La(Ba)	1.000*	0.855	0.694	0.629
Cu		1.000	0.500	0.634
O(1)			0.707	0.808
O(2)				0.851

The first column of Table VI lists our 44 best-fit parameters for La_2CuO_4. To obtain these, we weigh bands with energies between 0.51 and 0.59 Ry ten times as much as the other bands. This range brackets the LAPW Fermi level at 0.559 Ry, so that we obtain a particularly accurate fit there. The data for our fit include 17 bands at each of 71 k points from the LAPW results, with the addition of the 18th and 19th bands for a selected sample of k points to insure good representation of the La d states. The overall fitting error is 13.3 mRy, with bands 14–17 being less than 10 mRy off. Figure 2 compares the SK and LAPW band structure for La_2CuO_4. Near the Fermi energy, the fit is excellent, with the crucial 17th band having an rms error of only 6 mRy. The lowest bands are less accurate, but are still in good agreement.

Using fewer parameters can yield an accurate band structure, since the Cu-O d-p hopping parameters are the most significant, but only at the expense of refitting. Merely setting equal to zero the other hopping parameters from Table VI markedly worsens the fit. Figure 3 illustrates a fit generated by using only Cu-d and O-p states, and a total of 17 parameters. In the top panel, the La d, and Cu s and p parameters have merely been removed, without refitting, and the band structure and Fermi level recalculated. The fit has clearly been degraded. In the bottom panel, we have refit the data, restoring the accuracy of the bands near E_F, and even doing a reasonable job far below the Fermi level. The 17 parameters obtained this way are also listed in the middle column of Table VI. The total DOS generated by many- and few-parameter fits are compared in Fig. 4. The top panel is the 44 parameter result, and the bottom the 17 parameter DOS. Both SK fits reproduce the correct Fermi level and the van Hove singularity just below it, but the fit with fewer parameters does not reproduce a prominent Cu$(3z^2-r^2)$ peak at 0.5 Ry, instead showing a steplike band edge. This is probably a consequence of the resulting increase in two dimensionality of the bands, and indicates that simplified few-parameter TB parametrizations of these materials should be used with caution in making detailed

TABLE VI. Slater-Koster parameters (in Ry) for La_2CuO_4 and Ba_2CuO_4.

	La_2CuO_4; best fit (44 parameters)		La_2CuO_4; reduced set (17 parameters)		Ba_2CuO_4; best fit (44 parameters)		
			On-site parameters				
La:	t_{2g}	1.0869		Ba:	t_{2g}	1.4160	
	e_g	0.7679			e_g	1.2203	
O(1):	p	0.3359	0.2965	O(1):	p	0.3218	
O(2):	p	0.3954	0.3333	O(2):	p	0.4250	
Cu:	s	0.9930		Cu:	s	1.2717	
	p	1.4462			p	1.7015	
	t_{2g}	0.3581	0.3506		t_{2g}	0.2356	
	e_g	0.4592	0.4375		e_g	0.3376	
			First-neighbor parameters				
La-La:	$dd\sigma$	−0.0215		Ba-Ba:	$dd\sigma$	−0.0899	
	$dd\pi$	0.0143			$dd\pi$	−0.1007	
	$dd\delta$	−0.0137			$dd\delta$	−0.0286	
La-Cu:	$dd\sigma$	−0.0112		Ba-Cu:	$dd\sigma$	−0.1635	
	$dd\pi$	−0.0019			$dd\pi$	0.0004	
	$dd\delta$	0.0019			$dd\delta$	−0.0149	
La-O(1):	$dp\sigma$	−0.0380		Ba-O(1):	$dp\sigma$	−0.0006	
	$dp\pi$	0.0754			$dp\pi$	0.1210	
La-O(2):	$dp\sigma$	0.1762		Ba-O(2):	$dp\sigma$	0.3142	
	$dp\pi$	0.1907			$dp\pi$	0.2910	
Cu-Cu:	$ss\sigma$	0.0072		Cu-Cu:	$ss\sigma$	0.2086	
	$sp\sigma$	0.0056			$sp\sigma$	0.2489	
	$pp\sigma$	0.1685			$pp\sigma$	0.3395	
	$pp\pi$	−0.0930			$pp\pi$	−0.2689	
	$sd\sigma$	−0.0205			$sd\sigma$	−0.0321	
	$pd\sigma$	−0.0153			$pd\sigma$	−0.0378	
	$pd\pi$	0.0312			$pd\pi$	0.0537	
	$dd\sigma$	−0.0137	0.0048		$dd\sigma$	−0.0205	
	$dd\pi$	0.0031	−0.0049		$dd\pi$	0.0226	
	$dd\delta$	0.0028	−0.0058		$dd\delta$	−0.0051	
Cu-O(1):	$sp\sigma$	0.1849		Cu-O(1):	$sp\sigma$	0.1463	
	$pp\sigma$	−0.1831			$pp\sigma$	−0.1917	
	$pp\pi$	−0.0359			$pp\pi$	−0.0398	
	$dp\sigma$	0.1037	0.0921		$dp\sigma$	0.0807	
	$dp\pi$	0.0621	0.0631		$dp\pi$	0.0580	
Cu-O(2):	$sp\sigma$	0.0507		Cu-O(2):	$sp\sigma$	0.0747	
	$pp\sigma$	0.1163			$pp\sigma$	0.1313	
	$pp\pi$	0.0748			$pp\pi$	0.0769	
	$dp\sigma$	0.0507	0.0418		$dp\sigma$	0.0444	
	$dp\pi$	0.0318	0.0277		$dp\pi$	−0.0108	
O(1)-O(1):	$pp\sigma$	−0.0072	0.0431	O(1)-O(1):	$pp\sigma$	−0.0151	
	$pp\pi$	−0.0201	−0.0282		$pp\pi$	−0.0139	
O(1)-O(2):	$pp\sigma$	−0.0099	−0.0152	O(1)-O(2):	$pp\sigma$	−0.0239	
	$pp\pi$	−0.0271	−0.0144		$pp\pi$	−0.0168	
O(2)-O(2):	$pp\sigma$	0.0134	0.0126	O(2)-O(2)	$pp\sigma$	0.0063	
	$pp\pi$	−0.0001	−0.0018		$pp\pi$	0.0033	

predictions of their properties.

The decomposed DOS for La_2CuO_4 oxygen p states are shown in Fig. 5(a) and for copper d states are shown in Fig. 5(b). The σ direction for the in-plane oxygen O(1) points along the Cu-O(1) line, and the π direction is perpendicular to it. There is an extremely strong and narrow peak at 0.16 Ry for Cu(x^2-y^2), O(1) σ and O(1) π, indicative of the degree of oxygen-copper hybridization in these materials. Note also the van Hove singularity just below the Fermi level for Cu(x^2-y^2) and $(3z^2-r^2)$. From a rigid-band picture, one might speculate that substituting La with Ba, which has fewer electrons, could lower E_F into this singularity. We consider this in detail in Sec. III on our CPA study of the alloy.

An important comparison between our fit and the original LAPW results is the decomposition of the DOS near E_F. Table VII lists the decomposed DOS at the Fermi level and at the van Hove singularity below it. The SK

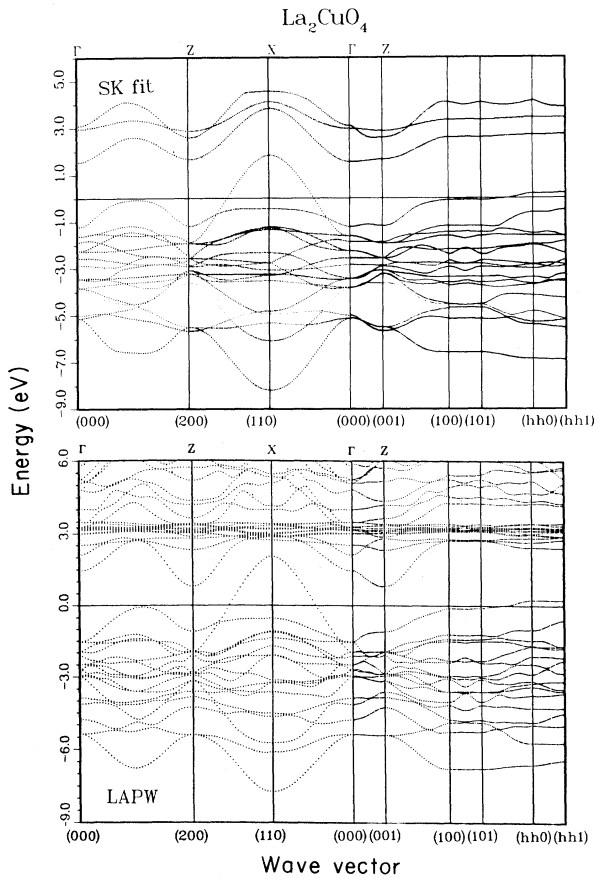

FIG. 2. La_2CuO_4: LAPW vs SK for the band structure. We have taken particular care to fit the bands near the Fermi level well.

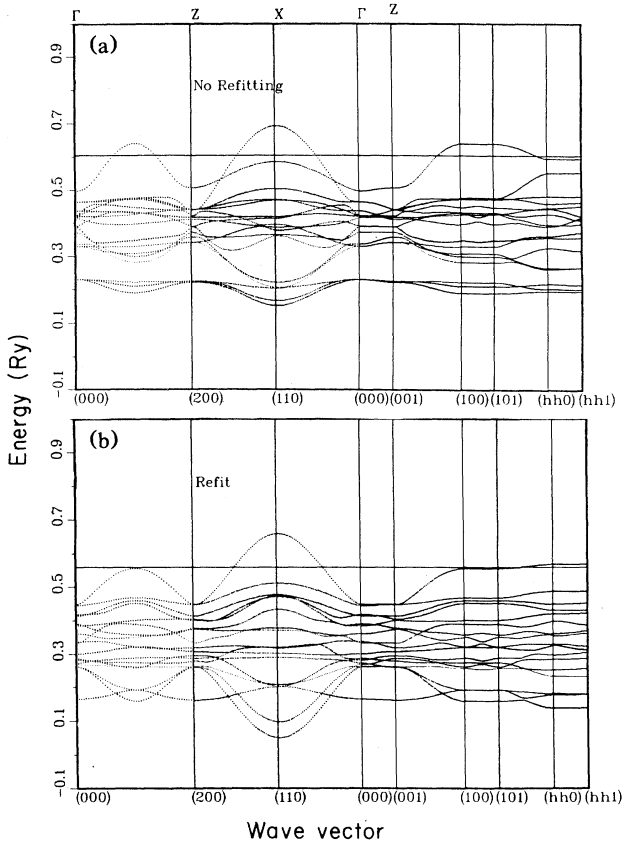

FIG. 3. La_2CuO_4: Effects on the SK fit of removing La d and Cu s and p parameters from the fit. (a) No refitting of SK parameters. (b) The 17 parameters were refit to the LAPW data. The accuracy of the bands has been largely restored.

Fermi level is 7 mRy below the LAPW value, and densities at E_F are 21.7 states/[Ry (unit cell)] for SK vs 16.0 states [Ry/(unit cell)] for LAPW. As for the decompositions, the LAPW result give 52% of the DOS at E_F in Cu-d, 21% in O(1)-p, and 8% O(2)-p, whereas the SK fit yields 72% Cu-d, 14% O(1)-p, and 6% O(2)-p. Considering our emphasis on fitting the bands rather than on fitting the decomposition, the agreement is quite good. The fit produces similarly good results at the van Hove singularity, which is 6 mRy lower in the SK than in the LAPW calculation. The DOS at the singularity is somewhat higher in the SK fit than the LAPW result, 44 states/(Ry cell) versus 29 states/(Ry cell), which may also account for the higher density at the Fermi level. The discrepancies are by no means drastic, and we expect our fits to be a good starting point for the disordered-state calculations.

Our Slater-Koster parameters compare reasonably with those obtained by McMahan, Martin, and Satpathy.[16] For example, for the on-site parameters they have Cu $d=0.34$ Ry, O(1) $p=0.25$ Ry, and O(2) $p=0.38$ Ry, in the units we use, adjusting for the difference in scale between their calculations and ours. By comparison, we have from Table VI Cu $t2g=0.35$ Ry, Cu $eg=0.44$ Ry, O(1) $p=0.30$ Ry, O(2) $p=0.33$ Ry. The hopping elements are less directly comparable, since we have many more than are used in the simple treatment of Ref. 16.

In order to do the alloy calculation, we also fit Ba_2CuO_4, using the same procedures outlined for the lanthanum compound. The parameters are listed in the third column of Table VI. The overall rms error for this ma-

TABLE VII. Comparison of total and partial DOS at the Fermi levels and van Hove singularities for Slater-Koster and LAPW for La_2CuO_4.

	Fermi level		van Hove	
	SK	LAPW	SK	LAPW
Energy (Ry)	0.552	0.559	0.546	0.552
Total DOS [states/(Ry cell)]	21.7	16.0	44.4	29.1
Partial DOS (% of total)				
Cu d	72	52	73	52
O(1) p	14	21	11	18
O(2) p	6	8	7	11

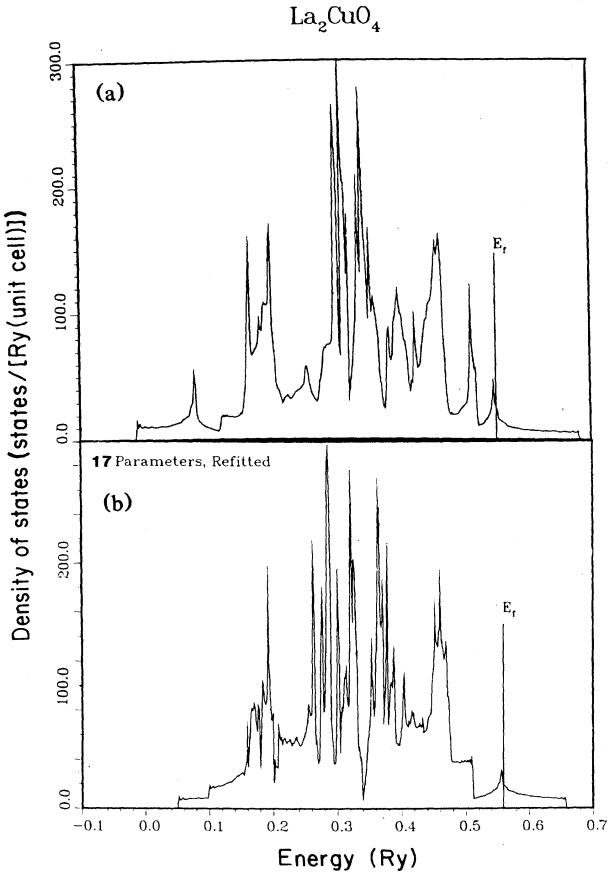

FIG. 4. La_2CuO_4: (a) Comparison of total DOS derived from our best SK fit (b) to that derived from the 17 parameter fit. Note the greater 2D character of the reduced parameter fit.

terial is 20 mRy, and the accuracy of the fit is similar to that of the lanthanum compound.

D. $YBa_2Cu_3O_7$

For this compound, we omit Ba and restrict the basis to Y-*d*, Cu-*d*, and O-*p* states, obtaining a 41×41 secular equation. We consider first-neighbor and the most important second- and third-neighbor hopping elements, so that the fit requires 79 SK parameters. The coordinates of the atoms are given in Table VIII, and the neighbor distances we use are given in Table IX. The structure is orthorhombic, with 13 atoms per unit cell distributed among eight distinct sites. For the lattice constants, we have $a=7.22495$ a.u., $b=1.01655a$, and $c=3.05599a$. The Cu-O planes consist of sites denoted Cu(2), O(2), and O(3), and the chain atoms are denoted Cu(1) and O(1). The O(4) sites lie between chain and plane copper atoms, but are much closer to the chain Cu(1) sites. As with the fit for the 2:1:4 compound, identical hopping elements are used for first and second or for second and third neighbors for which the neighbor distances were only slightly different.

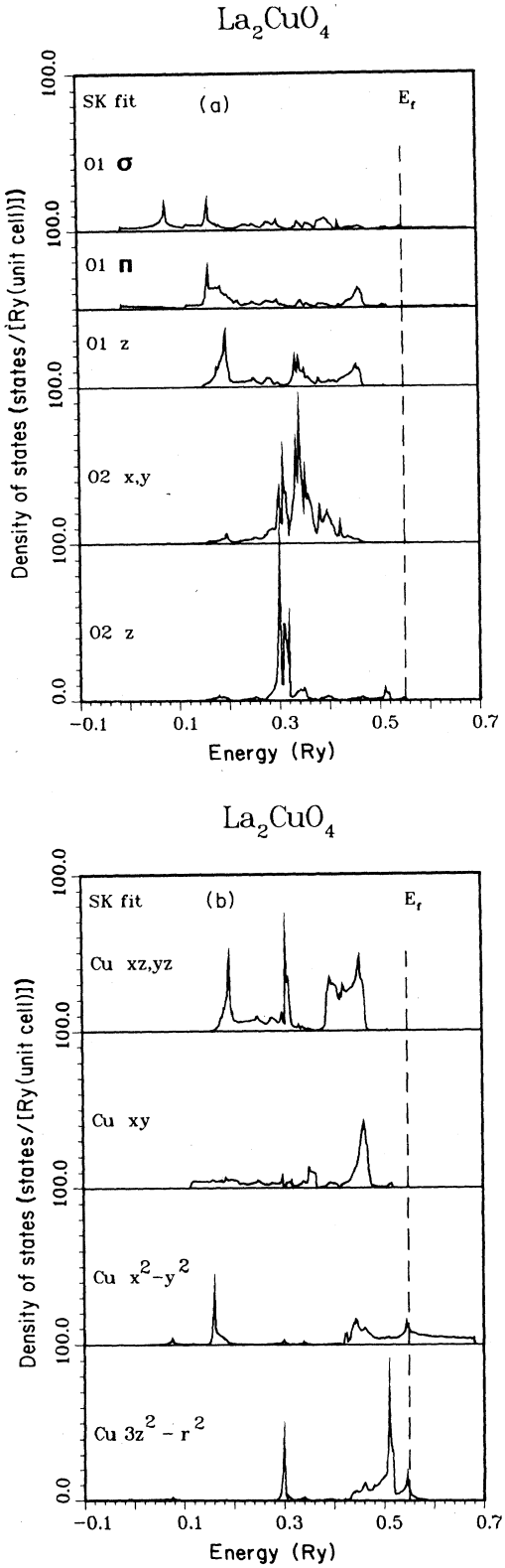

FIG. 5. (a) La_2CuO_4: Oxygen *p* DOS from the SK fit. The σ direction for the in-plane oxygen O(1) points toward Cu, and the π direction is perpendicular to it in the plane. The O(2) p_x and p_y densities are identical by symmetry. (b) La_2CuO_4: Copper *d* DOS from the SK fit.

TABLE VIII. Structure of $YBa_2Cu_3O_7$. $a=7.2249$ a.u., $b=1.01655a$, $c=3.05599a$.

Atom	x (units of a)	y (units of b)	z (units of c)	
Y	0.500	0.500	0.500	
Ba	0.500	0.500	0.1846	
Ba	0.500	0.500	0.8154	
Cu(1)	0.000	0.000	0.000	chain
Cu(2)	0.000	0.000	0.3551	plane
Cu(2)	0.000	0.000	0.6449	plane
O(1)	0.000	0.500	0.000	chain
O(2)	0.500	0.000	0.3781	plane
O(2)	0.500	0.000	0.6219	plane
O(3)	0.000	0.500	0.3779	plane
O(3)	0.000	0.500	0.6221	plane
O(4)	0.000	0.000	0.1579	
O(4)	0.000	0.000	0.8421	

In this compound, none of the atoms sits at sites of local cubic or even tetragonal symmetry. Thus, we have, in principle, crystal-field splittings for all the p and d bands. This is particularly important for Cu(1), which has a very asymmetric local environment. The splittings were negligible in 2:1:4 compounds, but must be considered here. Consequently, we describe O p on-site energies with three distinct values, and Cu d on-site energies with five distinct values. An additional difficulty arises from the sensitivity of the fit to the initial guesses for the TB parameters. Incorrect initial estimates can easily cause the program to iterate to incorrect local minima from which it cannot recover.

Our fitting data include 36–40 LAPW bands[17] at each of 165 k points throughout the Brillouin zone. The LAPW Fermi level is 0.442 Ry in our calculation, and LAPW eigenvalues in the range 0.4–0.6 Ry are given ten times the weight of values outside this range. Consequently, we have obtained a result in which the upper valence bands 24–36 are fit to within 10 mRy, with the Fermi-level-crossing bands 33–36 fit to within 5 mRy. Our best-fit parameters are listed in Table X. The bands are compared to the LAPW result in Fig. 6, with the zero of energy taken to be the LAPW Fermi level. The SK Fermi level almost exactly equals the LAPW value. We have sacrificed close agreement of the lower bands in order to fit the bands near E_F well. The total DOS's are compared in Fig. 7, which shows excellent agreement near the Fermi level. Again, there is a van Hove singularity below E_F, as in the 2:1:4 compound, but it consists of both quasi-2D Cu(1)-O(2),O(3) and quasi-1D Cu(1)-O(1) bands, and in the LAPW results is four times as far from the Fermi level as in the 2:1:4 compound. In the LAPW fit, it is 20 mRy below E_F, and in the SK fit it is 17 mRy below. Table XI compares the properties of the SK fit and the original LAPW results at the Fermi level and the van Hove singularity. The DOS at the Fermi level is 75.4 states/(Ry cell) in LAPW,[17] versus 66.1 states/(Ry cell) in the fit. The DOS at the singularity are 162 and 197 states/(Ry cell) in LAPW and SK, respectively. Thus, the total DOS near the Fermi level is reproduced very well by our fit. The decomposed DOS for copper and oxygen are plotted in Fig. 8. Aside from the O(4) p states having relatively little weight at E_F, the major discrepancy is that the planes have more weight relative to the chains in SK than in LAPW, 21% vs 39% for chains and 65% vs 40% for planes. However, as noted previously, very close agreement of the decompositions is not to be expected.

To illustrate our results further, we plot on an expanded scale bands near the Fermi level. Figure 9(a) shows the

TABLE IX. Yttrium, copper, and oxygen neighbors for $YBa_2Cu_3O_7$ (units of a). (* indicates that parameters for neighbors at $b=1.01655a$ were the same as for this neighbor.)

	First neighbors					
	Cu(1)	Cu(2)	O(1)	O(2)	O(3)	O(4)
Y	· · ·	0.8393	· · ·	0.6301	0.6305	· · ·
Cu(1)	1.000*	· · ·	0.5083	· · ·	· · ·	0.4825
Cu(2)		0.8856	· · ·	0.5049	0.5048	0.6026
O(1)			1.000*	· · ·	· · ·	0.7006
O(2)				0.7463	0.7130	0.8384
O(3)					0.7463	0.8427
O(4)						0.9651

	Second neighbors			
	Cu(2)	O(2)	O(3)	O(4)
Cu(2)	1.000*	0.9564	0.9613	· · ·
O(2)		1.000*	· · ·	· · ·
O(3)			1.000*	· · ·
O(4)				1.000*

	Third neighbors	
	O(2)	O(3)
Cu(2)	1.1350	1.1239

TABLE X. TB parameters for $YBa_2Cu_3O_7$. (Total of 79 parameters.)

		On-site parameters			
Y:	d	0.7322	O(1):	x	0.2530
Cu(1):	yz	0.3956		y	0.3071
	xz	0.3349		z	0.2878
	xy	0.2169	O(2):	x	0.2193
	x^2-y^2	0.2725		y	0.2909
	$3z^2-r^2$	0.3016		z	0.2249
Cu(2):	yz	0.3339	O(3):	x	0.3420
	xz	0.2652		y	0.1682
	xy	0.2390		z	0.2251
	x^2-y^2	0.2873	O(4):	x	0.1931
	$3z^2-r^2$	0.3446		y	0.3268
				z	0.2494
		First-neighbor parameters			
Y-Cu-(2):	$dd\sigma$	0.0564	Cu(2)-Cu(2):	$dd\sigma$	−0.0359
	$dd\pi$	−0.0360		$dd\pi$	−0.0173
	$dd\delta$	0.0376		$dd\delta$	−0.0200
Y-O(2):	$dp\sigma$	−0.0057	Cu(2)-O(2):	$dp\sigma$	0.0128
	$dp\pi$	0.0037		$dp\pi$	0.0842
Y-O(3):	$dp\sigma$	0.0077	Cu(2)-O(3):	$dp\sigma$	−0.0157
	$dp\pi$	0.0103		$dp\pi$	0.0565
Cu(1)-Cu(1):	$dd\sigma$	−0.0215	Cu(2)-O(4):	$dp\sigma$	−0.0110
	$dd\pi$	−0.0076		$dp\pi$	0.0302
	$dd\delta$	−0.0025	O(1)-O(1):	$pp\sigma$	0.0064
Cu(1)-O(1):	$dp\sigma$	0.0517		$pp\pi$	0.0109
	$dp\pi$	0.1035	O(1)-O(4):	$pp\sigma$	0.0123
Cu(1)-O(4):	$dp\sigma$	0.0542		$pp\pi$	0.0301
	$dp\pi$	0.0313	O(3)-O(3):	pps	−0.0552
O(2)-O(2):	$pp\sigma$	−0.0374		$pp\pi$	0.0033
	$pp\pi$	0.0442	O(3)-O(4):	$pp\sigma$	0.0606
O(2)-O(3):	$pp\sigma$	−0.0403		$pp\pi$	−0.0254
	$pp\pi$	0.0129	O(4)-O(4):	$pp\sigma$	−0.0325
O(2)-O(4):	$pp\sigma$	0.0433		$pp\pi$	0.0012
	$pp\pi$	0.0319			
		Second-neighbor parameters			
Cu(2)-Cu(2):	$dd\sigma$	−0.0160	O(2)-O(2):	$pp\sigma$	0.0145
	$dd\pi$	0.0259		$pp\pi$	−0.0103
	$dd\delta$	−0.0106	O(3)-O(3):	$pp\sigma$	−0.0017
Cu(2)-O(2):	$dp\sigma$	0.0069		$pp\pi$	−0.0086
	$dp\pi$	0.0150	O(4)-O(4):	$pp\sigma$	−0.0062
Cu(2)-O(3):	$dp\sigma$	0.0300		$pp\pi$	0.0083
	$dp\pi$	−0.0136			
		Third-neighbor parameters			
Cu(2)-O(2):	$dp\sigma$	−0.0240	Cu(3)-O(3):	$dp\sigma$	−0.0144
	$dp\pi$	0.0151		$dp\pi$	0.0048

$k_z=0$ plane and Fig. 9(b) the $k_z=0.5(2\pi/c)$ plane. The similarity of the two figures shows that bands near E_F are nearly 1D or 2D, somewhat more so in our fit than in the original LAPW result. Considering that we use relatively few parameters for this complicated structure, the fit is surprisingly good, reproducing not only the LAPW bands and total DOS, but also semiqualitatively fitting the angular momentum decomposition. The bands near E_F are accurate enough that our fit would reproduce most features of the Fermi surface, with discrepancies near the points (110) and (010).

III. CPA STUDY OF $La_{2-x}Ba_xCuO_{4-y}$

A. Introduction

The TB formalism allows us to reproduce one-electron properties of high-T_c superconductors accurately with a small and physically motivated basis and a compact set of parameters. This allows us in turn to consider problems which would be too costly to study with *ab initio* formalisms. We present here the application of our SK fits to the problem of disorder, using the (TB CPA).[18] Two kinds of disorder are considered, the random substitution of bari-

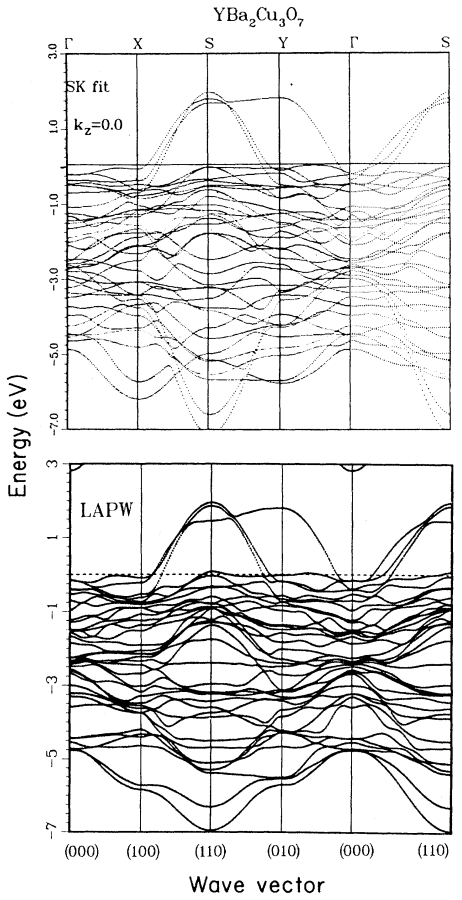

FIG. 6. $YBa_2Cu_3O_7$: LAPW vs SK for the band structure. Again, we have taken particular care to fit the bands near the LAPW Fermi level well.

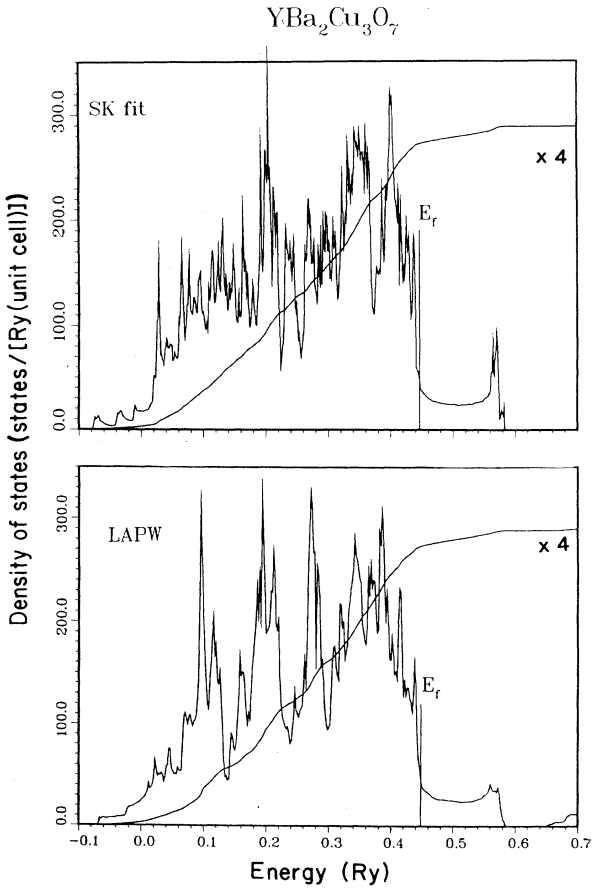

FIG. 7. $YBa_2Cu_3O_7$: LAPW vs SK for the total DOS. Near E_F, the DOS's are nearly identical.

TABLE XI. Comparison of Fermi levels and van Hove singularities for Slater-Koster and LAPW for $YBa_2Cu_3O_7$.

	Fermi level		van Hove	
	SK	LAPW[a]	SK	LAPW
Energy (Ry)	0.442	0.442	0.425	0.422
Total DOS [states/(Ry cell)]	66.1	75.4	197.2	162.4
Partial DOS (% of total)				
Cu(1) *d*	14	16	22	24
Cu(2) *d*	19	25	24	23
O(1) *p*	8	23	11	27
O(2) *p*	32	7	13	6
O(3) *p*	14	7	12	6
O(4) *p*	14	22	18	20
Total chain	21	39	33	51
Total plane	65	40	49	35

[a]Reference 17.

um for lanthanum, and random vacancies on the oxygen sites. Local atomic relaxations are ignored; in fact, they are not known.

The TB CPA is formulated as follows: The average effective medium is assumed to be periodic, so that the averaged single-particle retarded Green's function $G(R, R',z)=G(R-R',z)$, where R and R' are lattice vectors and z is the energy plus an infinitesimal imaginary part. $G(0,z)$ is then determined by inverting the TB k-space Schrödinger equation and averaging over the Brillouin zone

$$G(0,z)=\Omega^{-1}\int d^3k\,[z-H(k)]^{-1}, \tag{1}$$

where Ω is the zone volume, and $H(k)$ is the effective medium, $H(k)=[H_0(k)-\Sigma(k)]$. Here, H_0 is the unperturbed TB Hamiltonian, determined via the SK method, and $\Sigma(k)$ is the complex diagonal self-energy matrix, to be determined self-consistently by applying the CPA condition

$$0=\sum_j \langle t_j\rangle=\sum_j c_j(E_j-\Sigma)[1-(E_j-\Sigma)G(R=0,z)]^{-1}, \tag{2}$$

where E_j is the on-site (diagonal) matrix due to the jth

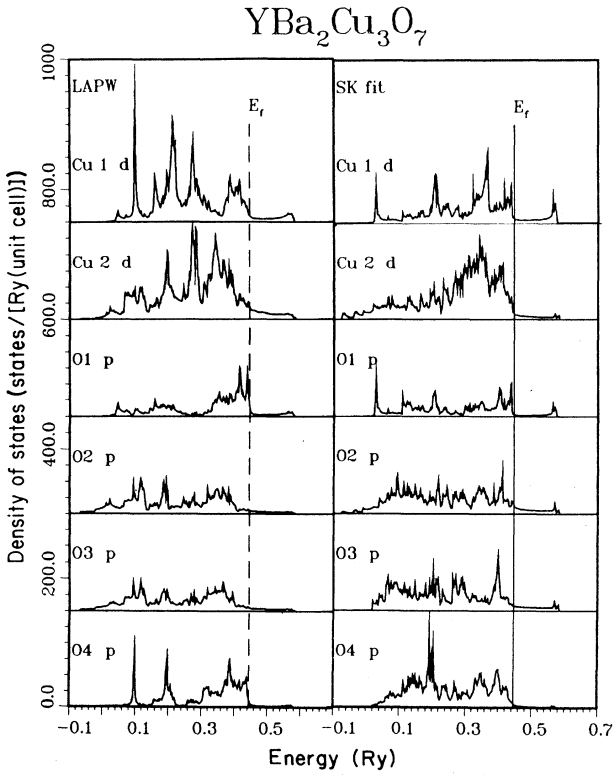

FIG. 8. $YBa_2Cu_3O_7$: LAPW vs SK decomposed DOS.

kind of impurity, t_j is the transition matrix, and c_j is the concentration. The DOS in energy $N(E)$ is found by taking the trace of G as the imaginary part of z vanishes:

$$N(E) = -(1/\pi)\,\mathrm{Im}[\mathrm{Tr}G(R=0,z=E^+)]\,, \qquad (3)$$

where the + indicates an infinitesimal positive imaginary part.

In our study, we neglect off-diagonal disorder, keeping the hopping elements at their values for pure La_2CuO_4. We also neglect shifts in the site energies of atoms neighboring the impurities. This approximation is inherent in the single-site CPA, but such shifts may have appreciable effects in materials with ionic character such as the copper oxides show.

A brief report on our work has appeared in Ref. 6, and we present here more details of the calculation.

B. $La_{2-x}Ba_xCuO_4$

The starting point for this calculation is the separate SK fits for La_2CuO_4 and Ba_2CuO_4. We take the lanthanum compound to be the unperturbed system, and its Fermi level sets the energy scale. An uncertainty then exists as to where to put the zero of energy of the barium compound (i.e., how to place its energy scale with respect to that of La_2CuO_4), since it has only 31 electrons per unit cell, compared to the lanthanum compound's 33. Instead of matching the two Fermi levels, we shift the site energies of Ba_2CuO_4 by 0.1 Ry so that the level at which its DOS would accommodate 33 electrons matches the lanthanum compound's Fermi level. This should be the appropriate starting point when the barium concentration is low. The two SK DOS are compared in Fig. 10. Both have van Hove singularities just below the 33 electron level, and they have similar values for $N(E_F)$. The major difference between the two is that the DOS for Ba_2CuO_4 almost has a gap near 0.2 Ry, but this feature is so far below the Fermi level that it should have no effect on the alloy DOS at E_F.

From a rigid-band picture, which may be expected to be reasonable when substituting similar atoms, one would expect that the effect of alloying would be to lower the Fermi level. The reason for this is that the two pure compounds have very similar DOS, especially near E_F. Thus, the alloy DOS should be substantially the same as that of La_2CuO_4 for small x. However, this DOS would have to accommodate not 33 electrons (La_2CuO_4) or 31 electrons (Ba_2CuO_4), but $(33-x)$, so that the Fermi level would fall below that for pure La_2CuO_4. This picture is in fact verified by our CPA results.

We consider $x=0.14$. Experimentally, superconductivity is first observed for $x=0.06$, and T_c reaches a maximum of 30 K for $x=0.15$.[11] The CPA DOS for $x=0.14$ is shown in Fig. 11. The van Hove singularity just below E_F has been broadened slightly, and the Fermi level has lowered near it. The effect of this is to increase the DOS at the Fermi level by 75%, as Table XII shows. Though we had expected the lowering of E_F, there had been the possibility that impurity broadening would wash out the van Hove singularity, leading to no significant change in $N(E_F)$. This is clearly not the case in our calculation, which in fact shows relatively little impurity broadening. Major peaks of the pure La_2CuO_4 DOS are clearly identifiable in the alloy DOS, and shift or attenuate little, validating the rigid-band picture.

The significance of this result for superconductivity should not be overlooked, since raising the DOS at the Fermi level enhances T_c for any superconductivity mechanism which pairs quasiparticles at E_F.

C. La_2CuO_{4-y}

In our work, we consider oxygen vacancies as a problem separate from La-Ba disorder. However, experimentally they occur together.[19] For small x (<0.15), y is typically less than 0.03, but for larger values of x, y increases, to nearly 0.10 for $x=0.3$. One common guess[19] as to the effect of removing oxygen is that it would cause the Fermi level to rise. The reasoning behind this guess is that each O site is initially occupied by an O^{2-} ion (or nearly so), so that removing a neutral O atom leaves behind two electrons which are "dumped" into the bands. Thus, oxygen vacancies might negate the enhancement of $N(E_F)$ by raising the Fermi level out of the van Hove singularity into which Ba substitution tends to drop it.

For the sake of simplicity, we take oxygen vacancies to randomly occupy both types of oxygen sites. We model vacancies as sites with infinite site energies, prohibiting

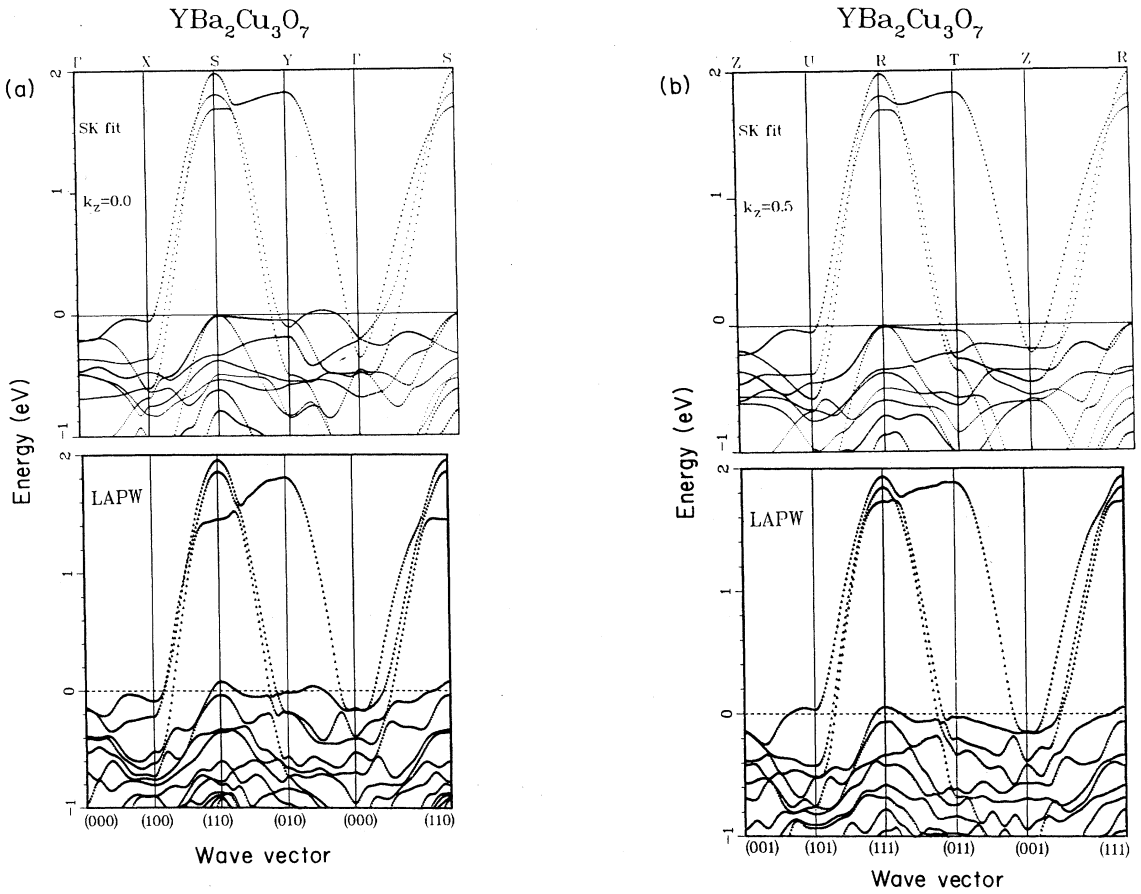

FIG. 9. (a) $YBa_2Cu_3O_7$: Comparison of bands near the Fermi level in the $k_z=0$ plane. (b) $YBa_2Cu_3O_7$: Comparison of bands near the Fermi level in the $k_z=0.5(2\pi/c)$ plane. The similarity of this figure to the one preceding indicates the degree to which the bands are 1D and 2D.

hopping to them. This gives a scattering matrix for the vacancies of $t_{\text{vac}}=-G^{-1}$, and should raise some of the DOS to infinite energy, effectively removing it from the system. We also continue to neglect off-diagonal disorder. The reason for this approximation is that though vacancy sites have much higher energies than the O sites, there are still vacancy orbitals. *A priori,* we do not know the matrix elements for hopping to these orbitals. However, in a disordered effective medium they will have some average values reflecting the disorder. For small vacancy concentrations, these values will be near those for the pure material, hence our (standard) approximation of neglecting off-diagonal disorder. Relaxing this approximation would require a much more complex formalism, such as that of Blackman, Esterling, and Berk,[20,21] yet would probably yield little improvement of the results at low vacancy concentrations.

Surprisingly, the expected increase of E_F outlined above is *not* found in our calculation. Instead, the lowering of the DOS below E_F is much smaller than expected, so that E_F initially remains constant then actually *falls* as y increases. This is demonstrated in Fig. 12, which shows the CPA DOS for $y=0.04$, 0.40, and 2.0. At the two lower vacancy concentrations, the Fermi level drops slightly to approach the van Hove singularity. For $y=0.40$, the DOS at the Fermi level is nearly doubled. The DOS at E_F for $y=0.04$ and 0.4 are given in Table XII.

The shift in the DOS at the Fermi level contradicts the commonly held hypothesis discussed previously that small amounts of oxygen vacancies should negate the effects of barium substitution.

The value $y=2$ is unphysically large, but is included to show that E_F can be drastically affected by oxygen vacancies in our model. It also illustrates clearly the physics of the calculation. For $y=2$, eight oxygen electrons are removed from each unit cell. However, the lowering of the

TABLE XII. E_F and $N(E_F)$ for $La_{2-x}Ba_xCuO_{4-y}$, calculated from Eq. (3).

		E_F (Ry)	$N(E_F)$ [states/(Ry cell)]
$y=0$:	$x=0.00$	0.5590	16.7
	0.14	0.5545	29.2
$x=0$:	$y=0.04$	0.5589	17.5
	$y=0.40$	0.5489	30.3

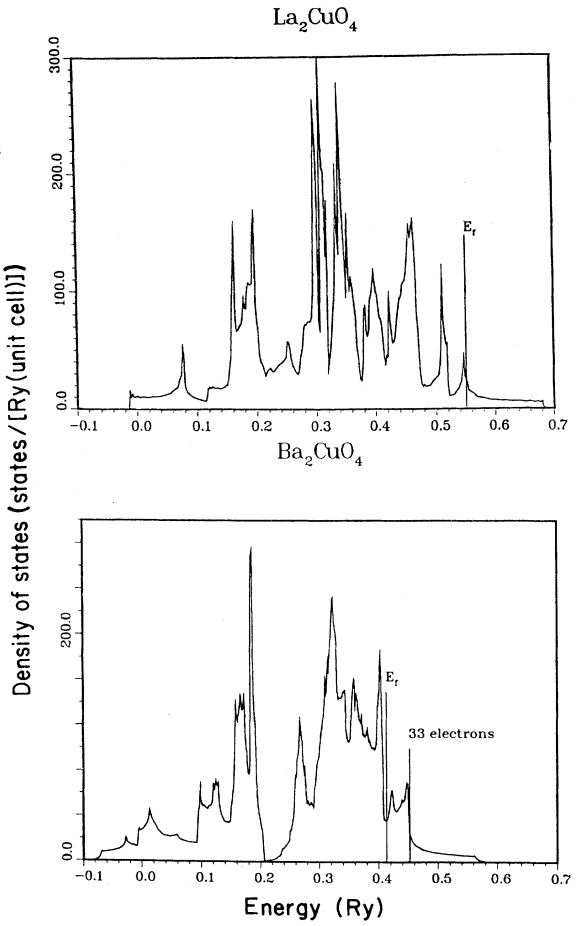

FIG. 10. La_2CuO_4 DOS vs Ba_2CuO_4 DOS. Near the level which would accommodate 33 electrons, the two are quite similar, indicating that rigid-band arguments should apply in the case of La-Ba substitution.

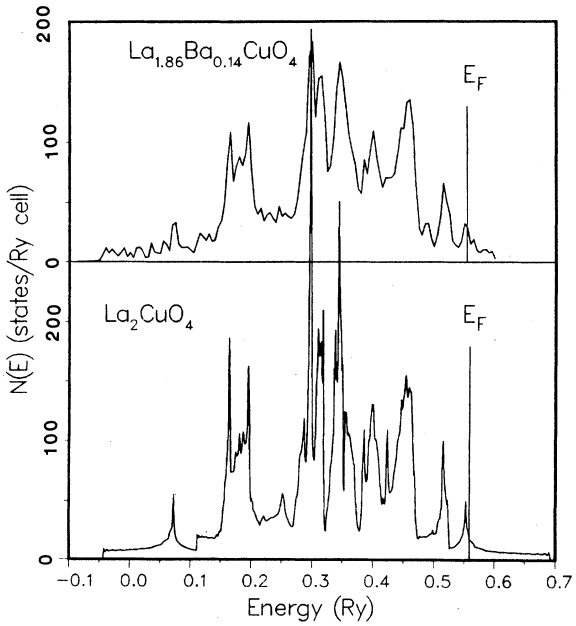

FIG. 11. $La_{2-x}BaCuO_4$: CPA DOS [Eq. (3)] for $x=0$ and $x=0.14$.

Fermi level is *not* a mere rigid-band effect. The 25 electron level for the $y=0$ case lies at 0.42 Ry, well below the new Fermi level. The new level is consistent with approximately seven states having been removed. This contrasts with the picture discussed above, in which 12 states would have been removed, causing E_F to rise. Physically, the electrons must adjust their propagation through the lattice to accommodate the vacancies. A plausible consequence of this is that the removal of oxygen leads to a narrowing of the broad Cu-O band straddling the Fermi surface.

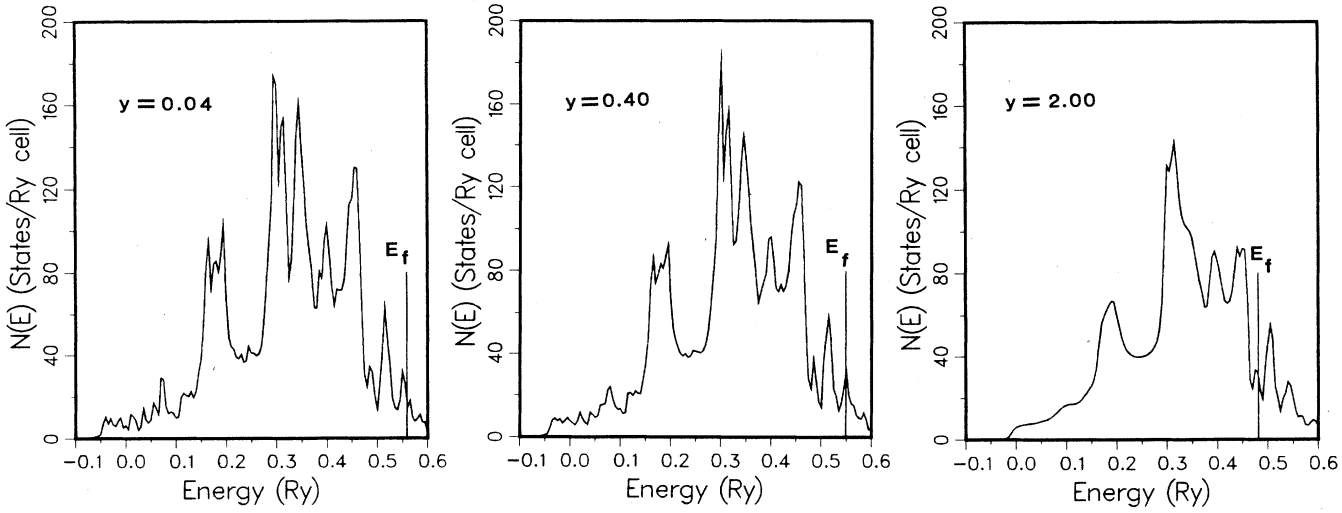

FIG. 12. La_2CuO_{4-y}: CPA DOS for values of y from 0.04 to 2.0. The largest y is unphysically large.

Some of the Cu atoms will be isolated, so that the density associated with them will resemble δ functions. The quasi-two-dimensional Cu-O planes will be more susceptible to this effect than more isotropic three-dimensional crystals would be. If the narrowing is greater than the disorder-induced broadening, it can bring down Cu density from above E_F, compensating partially for the loss of O density below E_F. This appears to be the case in our calculation. Further study on 1D and 2D binary compounds may give more insight into the essential physics of the vacancies.

The slight fall of the Fermi level at low vacancy concentrations may be related to the observation of trace superconductivity[22] in pure La_2CuO_4. This has been suggested to be due to understoichiometry of La,[23] or to excess oxygen.[24] However, our results show this may also be due to O vacancies enhancing $N(E_F)$.

IV. CONCLUSIONS

We have presented accurate, angular-momentum-decomposed TB parametrizations of high-temperature superconductors, and have used these within the CPA to produce the first calculations of the effects of disorder on the electronic structure of $La_{2-x}Ba_xCuO_{4-y}$. The results of our CPA calculations support the hypothesis of a rigid-band lowering of the Fermi level for $La_{2-x}Ba_x$-CuO_4, enhancing the DOS there. However, for La_2Cu-O_{4-y} they yield the unexpected result that oxygen vacancies *also* lower E_F and raise $N(E_F)$. This is a significant result for the theory of superconductivity in these materials. We are currently working to extend our CPA calculation to disordered $YBa_2Cu_3O_{7-y}$. This material, with 1D chain bands in addition to plane bands, should be even more susceptible to nonrigid-band effects of O vacancies than La_2CuO_4.

In any case, our parametrizations of the band structures should prove to be a useful tool for understanding these materials.

ACKNOWLEDGMENTS

We wish to thank H. Krakauer and R. E. Cohen, who participated in the LAPW band structure calculations and P. Pattnaik for valuable comments. This work was partially supported by the Office of Naval Research. One of us, M. J. DeWeert, acknowledges support through the Office of Naval Technology.

[1]W. E. Pickett, H. Krakauer, D. A. Papaconstantopoulos, and L. L. Boyer, Phys. Rev. B **35**, 7252 (1987).

[2]H. Krakauer and W. E. Pickett, in *Novel Superconductivity, Proceedings of the First International Conference on Novel Mechanisms of Superconductivity,* edited by V. Z. Kresin and S. A. Wolf (Plenum, New York, 1987).

[3]A. J. Freeman, J. Yu, and C. L. Fu, Phys. Rev. B **36**, 7111 (1987).

[4]L. F. Mattheiss, Phys. Rev. Lett. **58**, 1028 (1987).

[5]A review of the properties of this material are contained in D. R. Clarke, Adv. Ceram. Mater. **2**, 273 (1987).

[6]D. A. Papaconstantopoulos, W. E. Pickett, and M. J. DeWeert, Phys. Rev. Lett. **61**, 211 (1988).

[7]W. Weber, Phys. Rev. Lett. **58**, 1371 (1987).

[8]D. M. Newns, P. Pattnaik, M. Rasolt, and D. A. Papaconstantopoulos, Phys. Rev. B **38**, 7033 (1988).

[9]M. Inoue, T. Takemori, K. Ohtaka, R. Yoshizaki, and T. Sakudo, Solid State Commun. **63**, 201 (1987).

[10]V. Z. Kresin, Phys. Rev. B **35**, 8716 (1987).

[11]H. Takagi, S. Uchida, K. Kitazawa, and S. Tanaka, Jpn. J. Appl. Phys. **58**, 1035 (1987).

[12]A. Svane and O. Gunnarsson, Europhys. Lett. **7**, 171 (1988).

[13]J. C. Slater and G. F. Koster, Phys. Rev. **94**, 1498 (1954).

[14]D. A. Papaconstantopoulos and L. L. Boyer, in *Novel Superconductivity, Proceedings of the First International Conference on Novel Mechanisms of Superconductivity,* edited by V. Z. Kresin and S. A. Wolf (Plenum, New York, 1987).

[15]D. A. Papaconstantopoulos, M. J. DeWeert, and W. E. Pickett, in *High-Temperature Superconductors, 1988,* edited by M. B. Brodsky, R. C. Dynes, K. Kitazawa, and H. L. Tuller, Materials Research Society Symposia Proceedings, Vol. 99 (Materials Research Society, Pittsburgh, 1988), p. 447.

[16]A. K. McMahan, R. M. Martin, and S. Satpathy, Phys. Rev. B **38**, 6650 (1988).

[17]H. Krakauer, W. E. Pickett, and R. E. Cohen, J. Supercond. **1**, 111 (1988).

[18]J. S. Faulkner, Prog. Mater. Sci. **27**, 1 (1987).

[19]See the review by J. D. Jorgenson, in *Proceedings of the Eighteenth International Conference on Low-Temperature Physics (LT-18)* [Jpn. J. Appl. Phys. **26**, Suppl. 26-3, 2017 (1987)].

[20]J. A. Blackman, D. M. Esterling, and N. F. Berk, Phys. Rev. B **4**, 2412 (1971).

[21]A. Gonis and J. W. Garland, Phys. Rev. B **16**, 1495 (1977).

[22]P. M. Grant, S. S. P. Parkin, V. Y. Lee, E. M. Engler, M. L. Ramirez, J. E. Vasquez, G. Lim, R. D. Jacowitz, and R. L. Greene, Phys. Rev. Lett. **59**, 2482 (1987).

[23]A. H. Davies and R. J. D. Tilley, Nature (London) **326**, 859 (1987).

[24]J. M. Tarascon, L. H. Greene, B. G. Baclay, W. R. McKinnon, P. Barboux, and G. W. Hull, in *Novel Superconductivity, Proceedings of the First International Conference on Novel Mechanisms of Superconductivity,* edited by V. Z. Kresin and S. A. Wolf (Plenum, New York, 1987).